Appl Nanosci (2017) 7:67–73
DOI 10.1007/s13204-016-0543-x

ORIGINAL ARTICLE

Molybdenum disulfide grafted titania nanotube arrays as high capacity retention anode material for lithium ion batteries

Tauseef Anwar[1] · Li Wang[1] · Rizwan Ur Rehman Sagar[3] · Farhat Nosheen[4] · Khurram Shehzad[5] · Naveed Hussain[1] · Liang Tongxiang[2,6]

Received: 7 December 2016 / Accepted: 15 December 2016 / Published online: 30 December 2016

Abstract Titania nanotube arrays (TNAs) were grown by anodic oxidation method, and molybdenum disulfide (MoS_2) grafted TNAs have been synthesized via one-step hydrothermal process. The MoS_2 grafted TNAs (MoS_2/TNAs) when employed as an anode material in lithium ion battery, exhibited excellent areal specific capacity ($\sim$430 μAh cm^{-2}) at current density of 50 μA cm^{-2}, which is 33% higher as compared to the pure anatase TNAs and 55% higher as compared to MoS_2. Moreover, the capacity loss per cycle of MoS_2/TNAs ($\sim$0.21%) was significantly lower than anatase TNAs ($\sim$1.47%), suggesting an increase of capacity retention.

Keywords Molybdenum disulfide · Titanium dioxide nanotube arrays · Anode material · Lithium-ion batteries

Introduction

Lithium-ion batteries (LIBs) are not only attractive practical renewable energy storage devices for high-energy systems such as electrical vehicles, smart grids, etc., (Lu et al. 2013; Peterson et al. 2010; Thackeray et al. 2012) but they also fulfil the need of low energy gadgets such as PC memory, medical implants etc. (Armand and Tarascon 2008; Hu et al. 2010; Kyerematen 2014). Anode materials of LIBs have a significant effect on the overall performance and efficiency of LIBs (Shehzad et al. 2016; Sagar et al. 2016). However, anode materials for LIBs currently suffer from disadvantages such as, slow ionic diffusion, weak electron transportation, and high interface resistance, which consequently limits the performance of LIBs (Thackeray et al. 2012).

Titanium dioxide (TiO_2) is one of the attractive anode materials for LIBs due to its cost-effectiveness, chemical stability, and non-toxic nature. Various kinds of low dimensional TiO_2 such as nanotubes (Armstrong et al. 2006; Qiu et al. 2010), nanowires (Cao et al. 2010), nanorods (Liu et al. 2012), and nanoparticles (Ren et al. 2012) etc., have been employed as anode for LIBs. Amongst these nanostructures of TiO_2 (Armstrong et al. 2006; Qiu et al. 2010; Cao et al. 2010; Liu et al. 2012; Ren et al. 2012; Wang et al. 2011), titanium dioxide nanotube arrays (TNAs) (Guo et al. 2012; Anwar et al. 2015; Tauseef Anwar et al. 2016) are more advantageous owe to higher specific surface area, porosity, and vertical alignment. The TNAs not only provide

Electronic supplementary material The online version of this article (doi:10.1007/s13204-016-0543-x) contains supplementary material, which is available to authorized users.

✉ Liang Tongxiang
txliang@tsinghua.edu.cn

1 Beijing Key Lab of Fine Ceramics, Institute of Nuclear and New Energy Technology, Tsinghua University, Beijing 100084, People's Republic of China

2 State Key Lab of New Ceramic and Fine Processing, Tsinghua University, Beijing 100084, People's Republic of China

3 Nanshan District Key Lab for Biopolymers and Safety Evaluation, College of Materials Science and Engineering, Shenzhen University, Shenzhen 518060, People's Republic of China

4 Sulaiman Bin-Abdullah Aba Al-Khail-Centre of Interdisciplinary Research in Basic Sciences (SA-CIRBS), International Islamic University, Islamabad, Pakistan

5 Department of Information Technology and Electronics, Zhejiang University, Hangzhou, People's Republic of China

6 School of Materials Science and Engineering, Jiangxi University of Science and Technology, Ganzhou 100084, Jiangxi, People's Republic of China

the short lithium ion diffusion path but also accommodate the volume expansion, as well as easy preparation in large scale and self-standing structure facilitates film fabrication (Wu et al. 2012). However, TNAs have lower areal specific capacity (Anwar et al. 2015) which can be improved by adopting different strategies such as, metal or non-metal element doping (Liu et al. 2008, 2009, 2014), annealing in different atmosphere (Lu et al. 2012), conductive coating (Wang et al. 2015), and by compositing with the higher capacity materials (Anwar et al. 2016).

Molybdenum disulfide (MoS_2) is an attractive material for the practical applications including hydrogen storage, (Chen et al. 2001; Ye et al. 2006) as catalysts, (Hinnemann et al. 2005; Lukowski et al. 2013) lubricants, (Chhowalla and Amaratunga 2000; Savan et al. 2000) double-layer capacitor (Cao et al. 2013; Soon and Loh 2007) as well as lithiun-ion batteries (Hwang et al. 2011; Stephenson et al. 2014; Feng et al. 2009; Li et al. 2009; Dominko et al. 2002). As an anode for lithium insertion/deinsertion, the volume of MoS_2 has no significant expansion due to its unique layered structure and weak inter-layer interaction (Sun et al. 2016). Moreover, voids/dislocations in disordered MoS_2 results in a significant increase in lithium capacity ($\sim$670 mAh g^{-1}) as well as overall performance of the LIBs (Shehzad et al. 2016; Hwang et al. 2011; Liu et al. 2014; Zhu et al. 2014; Hu et al. 2016; Cui et al. 2015) Different composite of MoS_2 with conductive materials (graphene, carbon nanotubes, etc.) have been synthesised for the use of anodes in LIBs. (Zhao et al. 2016; Cao et al. 2013; Hwang et al. 2014) Since, the assembly of layered materials into variety of morphologies such as, nanoarrays is still in infacny, hence, the making composite of MoS_2 with arrays of TiO_2 may prove an interesting choice.

In this article, MoS_2 grafted TNAs have been prepared as a new hybrid anode material in order to improve LIBs performance. The MoS_2/TNAs composites were fabricated via hydrothermal method and a high lithium stroage capacity of 430 μAh cm^{-2} has been observed. The magnitude of areal capacity of MoS_2/TNAs is $\sim$33 and $\sim$55% higher as compared to the anatase TNAs and MoS_2, respectively. Not only the specific capacity is enhanced but also a new morphology of MoS_2 also helped to achieve a higher capacity retension. Better electrochemical performace of MoS_2/TNAs indicates its utility arising from its novel hybrid structure.

Experimental section

Synthesis of MoS_2/TNAs

MoS_2 grafted TNAs were synthesized according to the previous literature by using hydrothermal method (Fig. 1) (Anwar et al. 2015, 2016). The Ti-foil with grown TNAs was placed with top surface downward in the Teflon liner wall. The 30 mL solution of $(NH_4)_6Mo_7O_{24}{\cdot}4H_2O$ (1 mmol) and thiourea (H2NCSNH2 $\sim$ 0.484 g) was poured into the autoclaves which was Teflon lined. This sealed autoclave placed in oven for 3 h at the temperature of 180 °C. The autoclave was cooled down to room temperature. After cleaning samples were dehydrated at 80 °C for 30 min in vacuum oven. Annealing of MoS_2 deposited TNAs (MoS_2/TNAs) sample was performed at 400 °C for 2 h in argon atmosphere.

Characterization

The morphology of TNAs and MoS_2/TNAs was characterized by using field emission scanning electron microscopy (FE-SEM LEO 1530). The confirmation of TNAs, MoS_2 and MoS_2/TNAs phases was performed by using Cu $K\alpha$ radiation ($\lambda = 0.15$ nm) of X-ray powder diffraction (Rigaku D/max). Raman spectroscopy of the anatase TNAs, MoS_2, MoS_2/TNAs was recorded on a HR800 micro-Raman spectrometer (Horiba Jobin–Yvon) using a 633 nm He–Ne laser.

Electrochemical characterization

The electrochemical properties of MoS_2/TNAs composite were assessed by using Li| MoS_2/TNAs half-cells. The coin cell (2032) was assembled in a glove box filled with argon. MoS_2/TNAs was used as cathode without additives, while lithium foil was used as the anode. The cell was ready for the measurement after inserting a separator of celgard 2300 between anode and cathode. The electrolyte of 1 M $LiPF_6$ was dissolved in 1:1 volumetric ratio mixture of dimethyl carbonate (DMC) and ethylene carbonate (EC). The galvanostatically discharge and charge were conducted between 0.005 and 3 V (vs. Li/Li^+) at Land battery test system at room temperature. The electrodes used for comparison (TNAs and MoS_2) were prepared and characterized at same parameters. The cyclic voltammetry (CV) measurement was recorded using electrochemical workstation (CHI660C, CH Instruments, Shanghai, PRC).

Results and discussion

The morphology of anatase TNAs and MoS_2/TNAs under SEM indicate the smooth, uniform, and vertically aligned TNAs. The top surface and lateral surface do not have any unwanted nanostructures (Fig. 2a–d). The length and average pore diameter of the TNAs was $\sim$3–5 μm and $\sim$80 nm, respectively. The MoS_2 was grafted at TNAs by hydrothermal reaction for different time durations (i.e. 0–10 h) and found excellent performance of the device at 3 h as the excessive coating hindered the ions and electrons movement (Anwar et al. 2016). The partially covered top

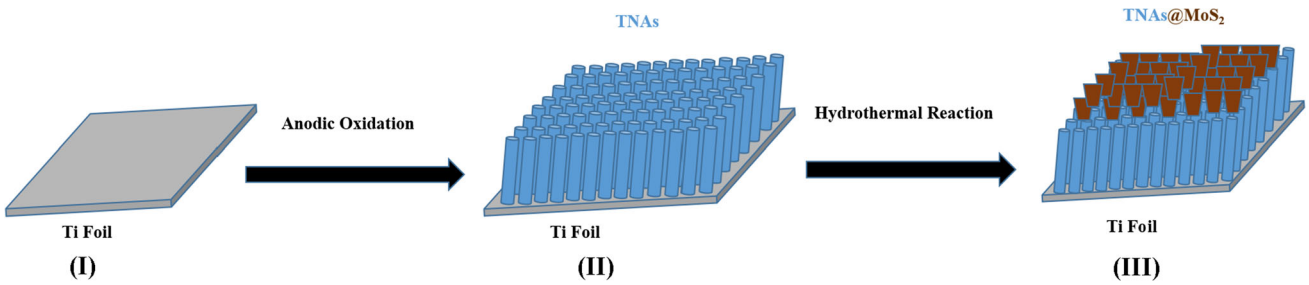

Fig. 1 The schematic diagram for MoS_2/TNAs composite fabrication: *I* Ti foil, *II* growth of TNAs at Ti foil, *III* MoS_2/TNAs fabrication

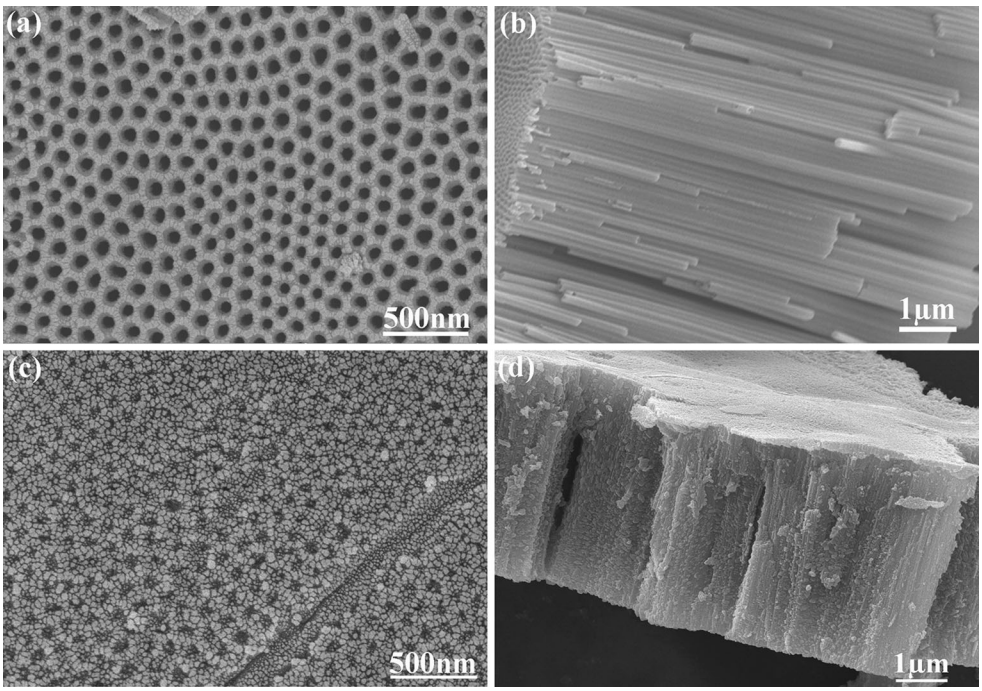

Fig. 2 **a** TNAs **c** MoS_2/TNAs and lateral side of **b** TNAs **d** MoS_2/TNAs

surface of TNAs with MoS_2 can facilitate Li ions and electrons movement through the inner of the nanotubes (Fig. 2c). The MoS_2 is also grafted at the lateral sides of TNAs (Fig. 2d), suggesting the filling of TNAs with MoS_2. The MoS_2 at bare titanium plate by similar method for 10 h is also shown in Fig. S1. The MoS_2 nanoflakes at titanium substrate are 500 nm long and 10 nm thick. The dimension of MoS_2 increases with the increase in the time.

The XRD peaks given in Fig. 3a indexed well with standard JCPDS No. 44-1294 and JCPDS No. 21-1272 for TNAs and MoS_2/TNAs, respectively. After MoS_2 coating the intensities of TiO_2 peaks decrease which indicates successful coating (Li et al. 2015). The peaks observed at 35°, 38.4°, 40.1°, 53°, 62.9°, 70.6°, 74.1°, 76.2° and 77.4° represents Ti foil planes while observed peaks at 14.38°, 29.03°, 33.51° and 62.81° can be attributed to MoS_2 (002), (004), (101), and (101) planes, respectively. Anatase-TiO_2 peaks were observed at 25.0° (101) and 47.9° (200). The MoS_2 peaks could be observed only in MoS_2/TNAs composite, and anatase TiO_2 did not show any MoS_2 peak. The XRD results suggest that anatase TNAs and MoS_2/TNAs are polycrystalline in nature.

The comparison of Raman spectra of anatase TNAs, MoS_2, and MoS_2/TNAs is performed for the investigation of the changes in the electronic structure (Fig. 3b). The intense Raman band at 145 cm^{-1} in MoS_2/TNAs corresponds to the main E_g vibration mode of anatase TiO_2. Moreover, the peaks located at 392 (B_{1g}), 513 (A_{1g}), and 634 cm^{-1} (E_g) also confirm the presence of anatase TiO_2. In MoS_2 spectrum, two broad peaks centered at 397 (E^1_{2g}) cm^{-1} and 406 (A_{1g}) cm^{-1} corresponds to the modes of MoS_2. The MoS_2 peaks are also observed in the Raman spectrum of the MoS_2/TNAs composites, confirming the successful coating of MoS_2 species on the anatase TNAs. The blue shift and peak broadening is observed in the mode of E_g, E_{1g}, A_{1g}, and E_g in the MoS_2/TNAs as compared to

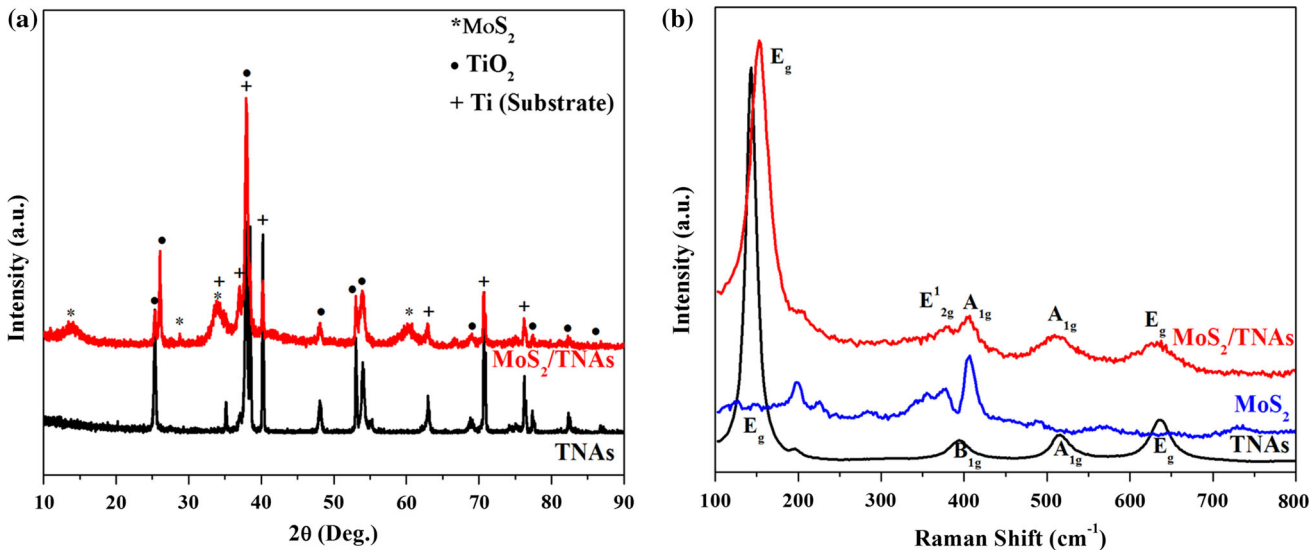

Fig. 3 **a** XRD and **b** Raman of TNAs, MoS_2 and MoS_2/TNAs

anatase TNAs. The blue shift might be attributed to the induced surface strain by the grafted MoS_2 nanoflakes at anatase TNAs surface (Fig. 4).

The cyclic voltammetry (CV) of all prepared electrodes were collected at scan rate of 5 mV/s in a potential window of 0.005–3 V vs. Li/Li^+ (Fig. 4a–c). The CV curve of anatase TNAs showed cathodic peaks at 1.2 and 1.35 V for 1st and 2nd cycle, respectively (Fig. 4a). Moreover, anodic peaks at 2.5 and 2.65 V correspond to the 1st and 2nd cycle of anatase TNAs, respectively, indicating the Li ion intercalation and de-intercalation potentials of the anatase TiO_2. The cathodic peak potentials are higher for 2nd cycle as compared to 1st cycle. The shoulder peak was observed at 0.2–1.0 V for both cycles with major peak, which depicted more lithium storage occurred at nanotubes surfaces and interfaces. The intensity of cathodic shoulder peak of the 2nd cycle is larger as compared to 1st cycle. Two cathodic/anodic peaks appeared at 0.6 V and 1.3 V (vs. Li/Li^+), respectively in the both cycles of MoS_2 anodes (Fig. 4b). The MoS_2/TNAs electrode showed the similar peaks of anatase TNAs cathodic peak and MoS_2 cycles behavior, indicating the contribution of TNAs and MoS_2 in MoS_2/TNAs anode (Fig. 4c). The whole Li^+ intercalation and deintercalation reaction can be described as:(Li et al. 2015)

$$TiO_2 + xLi^+ + xe^- \leftrightarrow Li_xTiO_2 \quad (1)$$

$$MoS_2 + xLi^+ + xe^- \rightarrow Li_xMoS_2 \quad (2)$$

$$Li_xMoS_2 + (4-x)Li^+ + (4-x)e^- \rightarrow Mo + 2Li_2S \quad (3)$$

The first two cycles were discharged/charged at 10 μA cm^{-2} to stabilize the electrochemical properties. The consecutive cycles (3rd–50th) were discharged/charged at current density of 50 μA cm^{-2} in the potential window of 0.005–3 V (Fig. 4d). In the 3rd discharge, the slope at 1.5–1.2 V corresponds to the TiO_2 lithiation. The slope after 1.0 V corresponded to the phase transformation from MoS_2 to Li_xMoS_2 and conversion into Mo and Li_2S (Eq. 3), respectively. The discharge capacity of 3rd cycle is 180, 290, and 430 μAh cm^{-2} for MoS_2, anatase TNAs and MoS_2/TNAs, respectively. The areal specific capacity of MoS_2/TNAs is higher as compared to MoS_2 and anatase TNAs. The improved electrochemical performance may be attributed to the synergistic effect of high capacity containing MoS_2 and vertically aligned nature of TNAs helps fast Li^+ kinetics.

To characterize stabilized electrochemical performance, first two discharged/charged were measured at the current density of 10 μA cm^{-2} (Fig. S2 (a) and (b)) while the remaining cycles were measured at 50 μA cm^{-2} (Fig. 5a). The cyclic stability of anatase TNAs reduces continuously from 3rd to 50th cycle with 1.47% capacity loss per cycle, while for MoS_2 cyclic performance is very stable from 3rd to 50th cycle with 0.08% capacity loss per cycle.

In the case of MoS_2/TNAs low capacity fading of TNAs is achieved and the capacity loss per cycle is just 0.21%. So it is an effective way to improve capacity retention. The composite electrode MoS_2/TNAs showed higher discharge/charge capacity as compared to individual anatase TNAs and MoS_2 electrodes. The MoS_2/TNAs nanostructures electrode exhibits a discharge capacity for 3rd cycle was 430 μAh cm^{-2} and low capacity fading until 50th cycle (388 μAh cm^{-2}) with capacity loss of 0.21% per cycle. While the discharge capacity of anatase TNAs and MoS_2 electrodes was 84 and 242 μAh cm^{-2} for 50th cycle, respectively. The efficiency of all electrodes is 100% during galvanostatic discharge/charge and fluctuates between 101 and 103% (Fig. 5a).

The rate performance was conducted at current densities of 50, 100, 150, 200, 250 and again 50 mA cm^{-2} for all

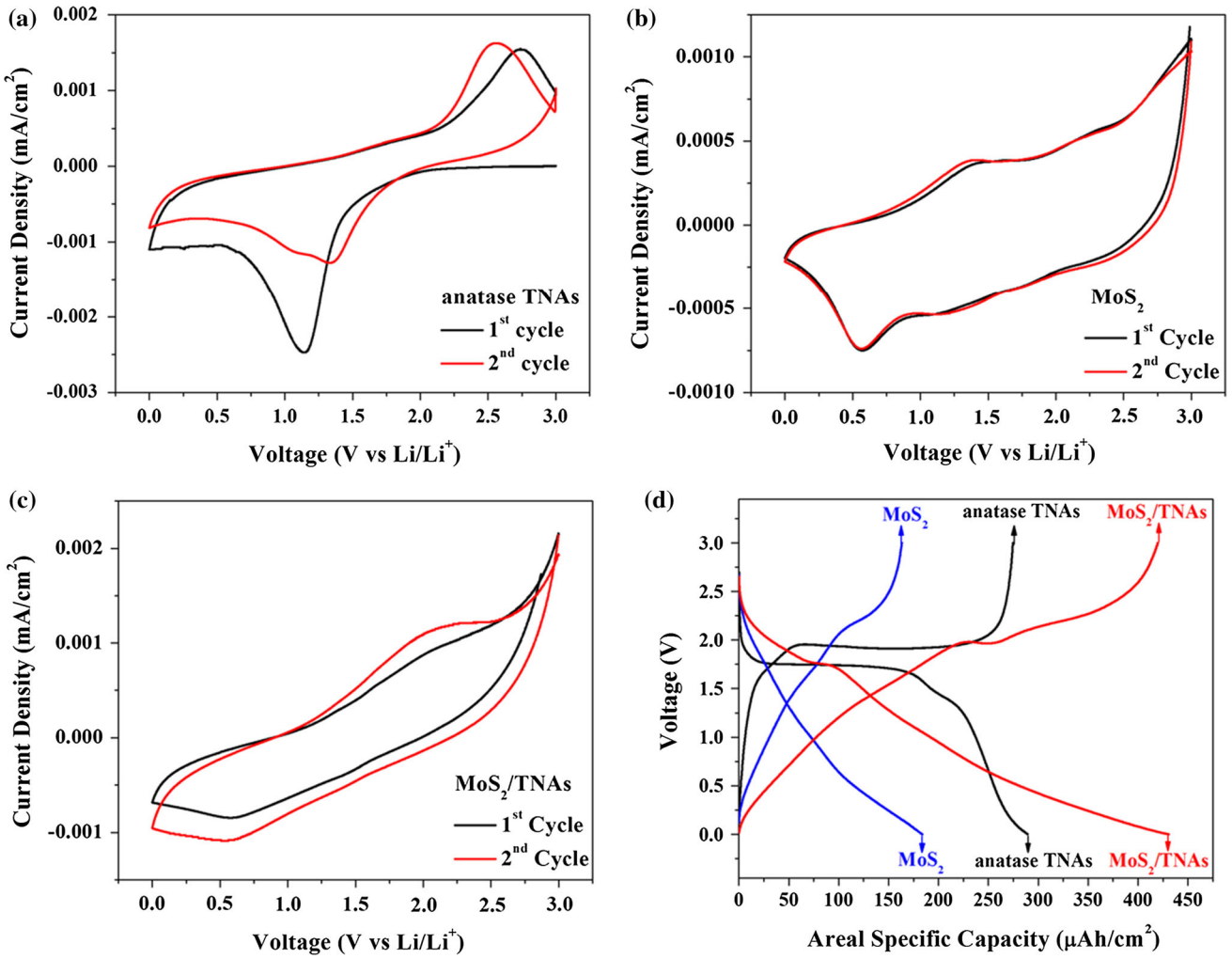

Fig. 4 CV curves for anatase TNAs (**a**), MoS_2 (**b**) and MoS_2/TNAs (**c**). **d** The 3rd galvanostatic discharge/charge curve of anatase TNAs, MoS_2 and MoS_2/TNAs at a potential of 0.005–3 V

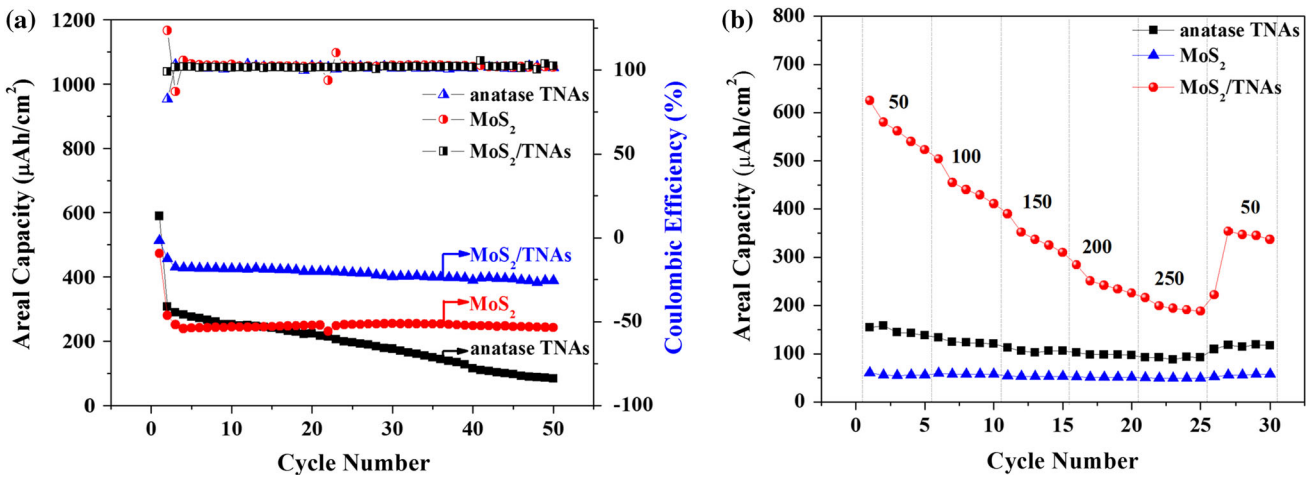

Fig. 5 Cyclic performance and efficiency (**a**) and rate performance (**b**)

electrodes. MoS_2/TNAs have high rate capability in comparison to anatase TNAs and MoS_2. At highest current density when discharge/charge rate switched again at 50 mA cm^{-2}, the areal capacity for MoS_2/TNAs was still more and stable as compared to anatase TNAs and MoS_2 (Fig. 5b). So the results depicted that TiO_2 and MoS_2 incorporate with each other and enhanced the lithium storage rate performance.

The MoS_2/TNAs can be a practical anode material in LIBs due to the achievement of larger areal capacity as well as high capacity retention. At First, there are no reports about MoS_2 grafted TNAs electrode for lithium ion battery and MoS_2 grafted TNAs of few micron length with higher specific capacity of 430 μAh cm^{-2}. It might be due to the fabrication process, nanostructures combination, and the synergetic effect of both nanostructured materials (i.e. MoS_2 and TNAs). The synergestic effect of MoS_2 and TNAs increased the lithium intercalation, which results into a higher capacity and better capacity retention. The hydrothermal fabrication helps to control MoS_2 thickness which brings the exciting performance and controllable performance of LIBs.

Conclusion

The electrochemical properties of MoS_2 nanoflakes grafted TNAs were studied for the first time to the best of our knowledge. The specific capacity (~430 μAh cm^{-2}) of MoS_2/TNAs is higher than anatase TNAs (~84 μAh cm^{-2}) and MoS_2 (~84 and 242 μAh cm^{-2}). Anatase TNAs have high capacity fading (i.e. 1.47% capacity loss/cycle), which was significantly reduced to 0.21% capacity loss/cycle, owing to the MoS_2 nanostructured coating over TNAs. Thus, MoS_2/TNAs material can be a promising anode material for lithium ion batteries.

Acknowledgements This work is supported by the National Natural Science Foundation of China (Grand No. 21271114); Tsinghua University independent research and development fund (20111080982) and Program for Changjiang Scholars and Innovative Research Team in University (IRT13026).

References

Anwar T, Wang L, Tongxiang L, He X, Sagar RUR, Shehzad K (2015) Effect of aspect ratio of titanium dioxide nanotube arrays on the performance of lithium ion battery. Int J Electrochem Sci 10(7):6537–6547

Anwar T, Wang L, Jiaoyang L, Chen W, Sagar RUR, Tongxiang L (2016) Lithium storage study on MoO_3-grafted TiO_2 nanotube arrays. Appl Nanosci 6(8):1–9

Armand M, Tarascon JM (2008) Building better batteries. Nature 451(7179):652–657

Armstrong G, Armstrong AR, Bruce PG, Reale P, Scrosati B (2006) TiO_2(B) nanowires as an improved anode material for lithium-ion batteries containing $LiFePO_4$ or LiNi0.5Mn1.5O4 cathodes and a polymer electrolyte. Adv Mater 18(19):2597–2600

Cao F-F, Wu X-L, Xin S, Guo Y-G, Wan L-J (2010) Facile synthesis of mesoporous TiO_2–C nanosphere as an improved anode material for superior high rate 1.5 V rechargeable Li ion batteries containing $LiFePO_4$–C cathode. J Phys Chem 114(22):10308–10313

Cao L, Yang S, Gao W, Liu Z, Gong Y, Ma L et al (2013a) Direct laser-patterned micro-supercapacitors from paintable MoS_2 films. Small 9(17):2905–2910

Cao X, Shi Y, Shi W, Rui X, Yan Q, Kong J et al (2013b) Preparation of MoS_2-coated three-dimensional graphene networks for high-performance anode material in lithium-ion batteries. Small 9(20):3433–3438

Chen J, Kuriyama N, Yuan H, Takeshita HT, Sakai T (2001) Electrochemical hydrogen storage in MoS_2 nanotubes. J Am Chem Soc 123(47):11813–11814

Chhowalla M, Amaratunga GAJ (2000) Thin films of fullerene-like MoS2 nanoparticles with ultra-low friction and wear. Nature 407(6801):164–167

Cui C, Li X, Hu Z, Xu J, Liu H, Ma J (2015) Growth of MoS_2@C nanobowls as a lithium-ion battery anode material. RSC Adv 5(112):92506–92514

Dominko R, Arčon D, Mrzel A, Zorko A, Cevc P, Venturini P et al (2002) Dichalcogenide nanotube electrodes for Li-ion batteries. Adv Mater 14(21):1531–1534

Feng C, Ma J, Li H, Zeng R, Guo Z, Liu H (2009) Synthesis of molybdenum disulfide (MoS_2) for lithium ion battery applications. Mater Res Bull 44(9):1811–1815

Guo W, Xue X, Wang S, Lin C, Wang ZL (2012) An integrated power pack of dye-sensitized solar cell and Li battery based on double-sided TiO_2 nanotube arrays. Nano Lett 12(5):2520–2523

Hinnemann B, Moses PG, Bonde J, Jørgensen KP, Nielsen JH, Horch S et al (2005) Biomimetic hydrogen evolution: MoS_2 nanoparticles as catalyst for hydrogen evolution. J Am Chem Soc 127(15):5308–5309

Hu L, Wu H, La Mantia F, Yang Y, Cui Y (2010) Thin, flexible secondary Li-ion paper batteries. ACS Nano 4(10):5843–5848

Hu Z, Liu Q, Sun W, Li W, Tao Z, Chou S-L et al (2016) MoS_2 with an intercalation reaction as a long-life anode material for lithium ion batteries. Inorg Chem Front 3(4):532–535

Hwang H, Kim H, Cho J (2011) MoS_2 nanoplates consisting of disordered graphene-like layers for high rate lithium battery anode materials. Nano Lett 11(11):4826–4830

Hwang M-J, Kim KM, Ryu K-S (2014) Effects of graphene on MoO_2–MoS_2 composite as anode material for lithium-ion batteries. J Electroceram 33(3):239–245

Kyerematen NA (2014) Self-organised TiO_2 nanotubes for 2D or 3D Li-ion microbatteries. Chemelectrochem 1:1442–1466

Li H, Li W, Ma L, Chen W, Wang J (2009) Electrochemical lithiation/delithiation performances of 3D flowerlike MoS_2 powders prepared by ionic liquid assisted hydrothermal route. J Alloys Compd 471(1–2):442–447

Li X, Li W, Li M, Cui P, Chen D, Gengenbach T et al (2015) Glucose-assisted synthesis of the hierarchical TiO_2 nanowire@MoS_2 nanosheet nanocomposite and its synergistic lithium storage performance. J Mater Chem A 3(6):2762–2769

Liu D, Xiao P, Zhang Y, Garcia BB, Zhang Q, Guo Q et al (2008) TiO_2 nanotube arrays annealed in N_2 for efficient lithium-ion intercalation. J Phys Chem C 112(30):11175–11180

Liu D, Zhang Y, Xiao P, Garcia BB, Zhang Q, Zhou X et al (2009) TiO_2 nanotube arrays annealed in CO exhibiting high performance for lithium ion intercalation. Electrochim Acta 54(27):6816–6820

Liu S, Jia H, Han L, Wang J, Gao P, Xu D et al (2012) Nanosheet-constructed porous TiO_2–B for advanced lithium ion batteries. Adv Mater 24(24):3201–3204

Liu Y, Zhao Y, Jiao L, Chen J (2014) A graphene-like MoS_2/-graphene nanocomposite as a highperformance anode for lithium ion batteries. J Mater Chem A 2(32):13109–13115

Lu Z, Yip C-T, Wang L, Huang H, Zhou L (2012) Hydrogenated TiO_2 nanotube arrays as high-rate anodes for lithium-ion microbatteries. Chempluschem 77(11):991–1000

Lu L, Han X, Li J, Hua J, Ouyang M (2013) A review on the key issues for lithium-ion battery management in electric vehicles. J Power Sources 226:272–288

Lü X, Yang W, Quan Z, Lin T, Bai L, Wang L et al (2014) Enhanced electron transport in Nb-Doped TiO_2 nanoparticles via pressure-induced phase transitions. J Am Chem Soc 136(1):419–426

Lukowski MA, Daniel AS, Meng F, Forticaux A, Li L, Jin S (2013) Enhanced hydrogen evolution catalysis from chemically exfoliated metallic MoS_2 nanosheets. J Am Chem Soc 135(28):10274–10277

Peterson SB, Apt J, Whitacre JF (2010) Lithium-ion battery cell degradation resulting from realistic vehicle and vehicle-to-grid utilization. J Power Sources 195(8):2385–2392

Qiu Y, Yan K, Yang S, Jin L, Deng H, Li W (2010) Synthesis of size-tunable anatase TiO_2 nanospindles and their assembly into anatase@titanium oxynitride/titanium nitride–graphene nanocomposites for rechargeable lithium ion batteries with high cycling performance. ACS Nano 4(11):6515–6526

Ren Y, Liu Z, Pourpoint F, Armstrong AR, Grey CP, Bruce PG (2012) Nanoparticulate TiO_2(B): an anode for lithium-ion batteries. Angew Chem Int Ed 51(9):2164–2167

Sagar RUR, Mahmood N, Stadler FJ, Anwar T, Navale ST, Shehzad K et al (2016) High capacity retention anode material for lithium ion battery. Electrochim Acta 211:156–163

Savan A, Pflüger E, Voumard P, Schröer A, Simmonds M (2000) Modern solid lubrication: recent developments and applications of MoS_2. Lubr Sci 12(2):185–203

Shehzad K, Xu Y, Gao C, Duan X (2016) Three-dimensional macro-structures of two-dimensional nanomaterials. Chem Soc Rev 45(20):5541–5588

Soon JM, Loh KP (2007) Electrochemical Double-layer capacitance of MoS_2 nanowall films. Electrochem Solid State Lett 10(11):A250–A254

Stephenson T, Li Z, Olsen B, Mitlin D (2014) Lithium ion battery applications of molybdenum disulfide (MoS_2) nanocomposites. Energy Environ Sci 7(1):209–231

Sun X, Wang Z, Li Z, Fu YQ (2016) Origin of structural transformation in mono- and bi-layered molybdenum disulfide. Sci Rep 6:26666

Tauseef Anwar WL, Hussain N, Chen W, Sagar RUR, Tongxiang L (2016) Effect of annealing atmosphere induced crystallite size changes on the electrochemical properties of TiO_2 nanotubes arrays. J Electr Eng 4:43–51

Thackeray MM, Wolverton C, Isaacs ED (2012) Electrical energy storage for transportation-approaching the limits of, and going beyond, lithium-ion batteries. Energy Environ Sci 5(7):7854–7863

Wang J, Zhou Y, Hu Y, O'Hayre R, Shao Z (2011) Facile synthesis of nanocrystalline TiO_2 mesoporous microspheres for lithium-ion batteries. J Phys Chem C 115(5):2529–2536

Wang XH, Guan C, Sun LM, Susantyoko RA, Fan HJ, Zhang Q (2015) Highly stable and flexible Li-ion battery anodes based on TiO_2 coated 3D carbon nanostructures. J Mater Chem A 3(30):15394–15398

Wu QL, Li J, Deshpande RD, Subramanian N, Rankin SE, Yang F et al (2012) Aligned TiO_2 nanotube arrays as durable lithium-ion battery negative electrodes. J Phys Chem C 116(35):18669–18677

Ye L, Wu C, Guo W, Xie Y (2006) MoS_2 hierarchical hollow cubic cages assembled by bilayers: one-step synthesis and their electrochemical hydrogen storage properties. Chem Commun 45:4738–4740

Zhao B, Wang Z, Gao Y, Chen L, Lu M, Jiao Z et al (2016) Hydrothermal synthesis of layer-controlled MoS_2/graphene composite aerogels for lithium-ion battery anode materials. Appl Surf Sci 390:209–215

Zhu C, Mu X, van Aken PA, Yu Y, Maier J (2014) Single-layered ultrasmall nanoplates of MoS_2 embedded in carbon nanofibers with excellent electrochemical performance for lithium and sodium storage. Angew Chem Int Ed 53(8):2152–2156